

The symmetry energy in nucleon and quark matter

Lie-Wen Chen^{*1,2}

¹*School of Physics and Astronomy and Shanghai Key Laboratory for Particle Physics and Cosmology, Shanghai Jiao Tong University, Shanghai 200240, China*

²*Center of Theoretical Nuclear Physics, National Laboratory of Heavy Ion Accelerator, Lanzhou 730000, China*

(Dated: July 28, 2021)

The symmetry energy characterizes the isospin dependent part of the equation of state of isospin asymmetric strong interaction matter and it plays a critical role in many issues of nuclear physics and astrophysics. In this talk, we briefly review the current status on the determination of the symmetry energy in nucleon (nuclear) and quark matter. For nuclear matter, while the subsaturation density behaviors of the symmetry energy are relatively well-determined and significant progress has been made on the symmetry energy around saturation density, the determination of the suprasaturation density behaviors of the symmetry energy remains a big challenge. For quark matter, which is expected to appear in dense matter at high baryon densities, we briefly review the recent work about the effects of quark matter symmetry energy on the properties of quark stars and the implication of possible existence of heavy quark stars on quark matter symmetry energy. The results indicate that the u and d quarks could feel very different interactions in isospin asymmetric quark matter, which may have important implications on the isospin effects of partonic dynamics in relativistic heavy-ion collisions.

PACS numbers: 21.65.Ef, 21.65.Cd, 21.65.Qr, 97.60.Jd, 25.75.-q

I. INTRODUCTION

The density dependence of nuclear matter symmetry energy $E_{\text{sym}}(\rho)$, which characterizes the isospin dependent part of the equation of state (EOS) of asymmetric nuclear matter, attracts much interest in current research frontiers of nuclear physics and astrophysics. The exact information on nuclear matter symmetry energy is critically important for understanding many challenging questions ranging from the structure of radioactive nuclei, the reaction dynamics induced by rare isotopes, the liquid-gas phase transition in asymmetric nuclear matter and the isospin dependence of QCD phase diagram to the location of neutron drip line and r-process paths in the nuclear landscape, the properties of neutron stars and the explosion mechanism of supernova as well as the frequency and strain amplitude of gravitational waves from inspiraling neutron star binaries [1–20]. In addition, some interesting issues of possible new physics beyond the standard model [21–24] may also be related to the symmetry energy.

While important progress has been made in recent years on constraining the density dependence of nuclear matter symmetry energy, mainly based on the data analysis from terrestrial laboratory measurements and astrophysical observations [3–13, 15–20] as well as some *ab initio* theoretical calculations [25], large uncertainties still exist, especially for its high density behaviors [26–30]. Accurate determination of the density dependence of nuclear matter symmetry energy thus provides a strong motivation for the investigation of isospin

nuclear physics at the new/planning radioactive isotope beam facilities around the world, such as CSR/Lanzhou and BRIF-II/Beijing in China, SPIRAL2/GANIL in France, FAIR/GSI in Germany, RIBF/RIKEN in Japan, SPES/LNL in Italy, RAON in Korea, and FRIB/NSCL and T-REX/TAMU in USA.

At extremely high baryon densities, the matter would become deconfined quark matter. Since isospin symmetry is still satisfied in quark matter, quark matter symmetry energy is thus involved for the properties of isospin asymmetric quark matter. The isospin asymmetric quark matter could exist in compact stars such as neutron stars or quark stars, and it could be also produced in heavy ion collisions induced by neutron-rich nuclei at ultra-relativistic energies. Although essential progress has been made in understanding the density dependence of nuclear matter symmetry energy, little empirical information is known on the density dependence of quark matter symmetry energy [31–37]. Theoretically, it is hard to evaluate the quark matter symmetry energy since the *ab initio* Lattice QCD simulations do not work at large baryon densities while model-independent perturbative QCD works only at extremely high baryon densities.

In the present paper, we briefly review the current status on the determination of the symmetry energy in nuclear and quark matter.

II. THE SYMMETRY ENERGY

The EOS of isospin asymmetric nuclear matter with baryon density $\rho = \rho_n + \rho_p$ (ρ_n and ρ_p denote the neutron and proton densities, respectively) and isospin asymmetry $\delta = (\rho_n - \rho_p)/(\rho_p + \rho_n)$, given by the binding energy

*email: lwchen@sjtu.edu.cn

per nucleon, can be expanded in δ as

$$E(\rho, \delta) = E_0(\rho) + E_{\text{sym}}(\rho)\delta^2 + O(\delta^4), \quad (1)$$

where $E_0(\rho) = E(\rho, \delta = 0)$ represents the EOS of symmetric nuclear matter, and the nuclear matter symmetry energy is expressed as

$$E_{\text{sym}}(\rho) = \frac{1}{2!} \frac{\partial^2 E(\rho, \delta)}{\partial \delta^2} \Big|_{\delta=0}. \quad (2)$$

In Eq. (1), the disappearance of odd-order terms in δ is due to the exchange symmetry between protons and neutrons in nuclear matter when the electromagnetic interaction among nucleons is not considered. Neglecting the contribution from higher-order δ terms in Eq. (1) leads to the well-known empirical parabolic law for the EOS of asymmetric nuclear matter, which has been verified by many many-body theories to date, at least for densities up to moderate values [6, 38].

Around a reference density ρ_r , the $E_{\text{sym}}(\rho)$ can be expanded in $\chi_r = (\rho - \rho_r)/\rho_r$ as

$$E_{\text{sym}}(\rho) = E_{\text{sym}}(\rho_r) + \frac{L(\rho_r)}{3} \chi_r + O(\chi_r^2), \quad (3)$$

where $L(\rho_r) = 3\rho_r \frac{\partial E_{\text{sym}}(\rho)}{\partial \rho} \Big|_{\rho=\rho_r}$ is the density slope parameter at ρ_r which characterizes the density dependence of the symmetry energy around ρ_r . At saturation density ρ_0 of symmetric nuclear matter, $L(\rho_r)$ is reduced to $L \equiv L(\rho_0)$.

Similarly as for nuclear matter, the EOS of three-flavor u - d - s quark matter with baryon number density n_B , isospin asymmetry δ_q and s -quark number density n_s , defined by the binding energy per baryon number, can be also expanded in isospin asymmetry δ_q as

$$E(n_B, \delta_q, n_s) = E_0(n_B, n_s) + E_{\text{sym}}(n_B, n_s)\delta_q^2 + \mathcal{O}(\delta_q^4), \quad (4)$$

where $E_0(n_B, n_s) = E(n_B, \delta_q = 0, n_s)$ is the binding energy per baryon number in isospin-symmetric u - d - s quark matter with equal u and d fraction; the quark matter symmetry energy $E_{\text{sym}}(n_B, n_s)$ is expressed as

$$E_{\text{sym}}(n_B, n_s) = \frac{1}{2!} \frac{\partial^2 E(n_B, \delta_q, n_s)}{\partial \delta_q^2} \Big|_{\delta_q=0}. \quad (5)$$

The isospin asymmetry of quark matter is defined as

$$\delta_q = 3 \frac{n_d - n_u}{n_d + n_u}, \quad (6)$$

which equals to $-n_3/n_B$ with the isospin density $n_3 = n_u - n_d$ and $n_B = (n_u + n_d)/3$ for two-flavor u - d quark matter. We note that the above definition of δ_q for quark matter has been extensively used in the literature [31–37], and one has $\delta_q = 1$ (-1) for quark matter converted by pure neutron (proton) matter according to the nucleon constituent quark structure, consistent with the conventional definition for nuclear matter, namely,

$\frac{\rho_n - \rho_p}{\rho_n + \rho_p} = -n_3/n_B$. In Eq. (4), the absence of odd-order terms in δ_q is due to the exchange symmetry between u and d quarks in quark matter when the electromagnetic interaction among quarks is not considered. The higher-order coefficients in δ_q are shown to be very small in various model calculations [35] and thus the empirical parabolic law is also approximately satisfied for the EOS of asymmetric quark matter.

III. NUCLEAR MATTER SYMMETRY ENERGY AROUND THE SATURATION DENSITY

Theoretically, it remains a big challenge to calculate the density dependence of nuclear matter symmetry energy, mainly due to our poor knowledge of nuclear (effective) interactions as well as the limitation of the present nuclear many-body techniques. As an example, shown in the left panel of Fig. 1 is the nuclear matter symmetry energy as a function of the density normalized by the corresponding saturation density ρ_0 with 60 well-calibrated interactions in various energy density functionals, namely, 18 nonlinear RMF interactions (FSUGold, PK1s24, NL3s25, G2, TM1, NL-SV2, NL-SH, NL-RA1, PK1, NL3, NL3*, G1, NL2, NL1, IU-FSU, BSP, IUFSU*, TM1*), 3 point-coupling RMF interactions (DD-PC1, PC-PK1, PC-F1), 2 relativistic HF interactions (PKO3 and PKA1), 2 density-dependent RMF interactions (DD-ME1 and DD-ME2), 2 Gogny interactions (D1S and D1N), and 33 Skyrme interactions (v090, MSk7, BSk8, SKP, SKT6, SKX, BSk17, SGII, SKM*, SLy4, SLy5, MSkA, MSL0, SIV, SkSM*, kMP, SKa, Rsigma, Gsigma, SKT4, SV, SkI2, SkI5, BSK18, BSK19, BSK20, BSK21, MSL1, SAMi, SV-min, UNEDF0, UNEDF1, TOV-min). These interactions include the 46 interactions used in Ref. [39] (except BCP which is designed for density up to only 0.24 fm^{-3}) and other 14 interactions (i.e., BSK18, BSK19, BSK20, BSK21, MSL1, SAMi, SV-min, UNEDF0, UNEDF1, TOV-min, IU-FSU, BSP, IUFSU*, TM1*) constructed more recently. For more details, see Ref. [40]. Shown in the right panel of Fig. 1 are the results from some microscopic many-body approaches, namely, the non-relativistic Brueckner-Hartree-Fock (BHF) approach [41, 42], the relativistic Dirac-Brueckner-Hartree-Fock (DBHF) approach [43, 44], and the variational many-body (VMB) approach [45–47]. The result from the Skyrme interaction BSk21 is also included in the right panel of Fig. 1 for comparison. It is clearly seen that various theoretical models and approaches predict very different density behaviors of the symmetry energy, especially at supra-saturation densities, indicating the importance of experimental constraints on the density dependence of nuclear matter symmetry energy.

During the last decade, a number of experimental or observable probes have been proposed to constrain the density dependence of nuclear matter symmetry energy [6]. Most of them are for the symmetry energy

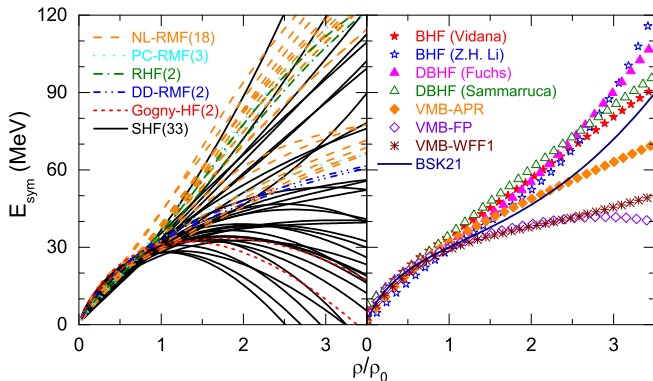


FIG. 1: (Color online) Nuclear matter symmetry energy as a function of the density normalized by the corresponding saturation ρ_0 from various energy density functionals with 60 interactions (Left panel) and microscopic many-body approaches (Right panel). See text for the details.

around saturation density while a few of probes are for the supra-saturation density behaviors. By analyzing the data from nuclear reactions, nuclear structures, and the properties of neutron stars based on various models or methods, more than 30 constraints, mainly on the parameters $E_{\text{sym}}(\rho_0)$ and L , have been obtained, see, e.g. Refs. [10, 13] for a summary. As indicated in Ref. [13], these constraints on $E_{\text{sym}}(\rho_0)$ and L cannot be equivalently reliable since some of them do not have any overlap at all. However, essentially all the constraints seem to agree with $E_{\text{sym}}(\rho_0) = 32.5 \pm 2.5$ MeV and $L = 55 \pm 25$ MeV.

The experimental probes of nuclear matter symmetry energy, especially those related to the structure properties of finite nuclei, generally depend on both $E_{\text{sym}}(\rho_0)$ and L . This is because the structure properties of finite nuclei are generally related to the subsaturation density behaviors of the symmetry energy due to the surface existence of finite nuclei, and a constraint of the symmetry energy at subsaturation density will generally lead to a correlation between $E_{\text{sym}}(\rho_0)$ and L at saturation density [48, 49]. Therefore, the constraints on nuclear matter symmetry energy around saturation density are usually plotted in the $E_{\text{sym}}(\rho_0)$ - L plane. As an example, shown in Fig. 2 are six typical experimental constraints on $E_{\text{sym}}(\rho_0)$ (denoted as S_v in Fig. 2) and L summarized by Lattimer and Steiner [50], namely, the constraint deduced from nuclear masses taken from Hartree-Fock calculations with the UNEDF0 density functional [51] (labeled “nuclear mass”), the constraint from Skyrme-Hartree-Fock analysis on the neutron skin thickness of Sn isotopes by Chen et al. [52] (labeled “Sn neutron skin”), the constraint from the electric dipole polarizability α_D of ^{208}Pb measured by Tamii et al. [53] (labeled “dipole polarizability”), the constraint from the centroid energy of the giant dipole resonance for ^{208}Pb taken from Trippa, Colo and Vigezzi [54] (labeled “GDR”),

the constraint from an improved quantum molecular dynamics (ImQMD) transport model analysis [55] of the isospin diffusion data from two different observables and the ratios of neutron and proton spectra in collisions at $E/A = 50$ MeV involving ^{112}Sn and ^{124}Sn (labeled “HIC”), and the constraint from the energies of excitations to isobaric analog states taken from Danielewicz and Lee [56] (labeled “IAS”). For more details on these constraints, see, Ref. [50]. The white region displayed in Fig. 2 represents the consensus agreement of the six experimental constraints above, giving quite precise values of $E_{\text{sym}}(\rho_0) = 31.5 \pm 1.0$ MeV and $L = 55 \pm 11$ MeV.

It is interesting to see from Fig. 2 that while other experimental constraints put a positive correlation between $E_{\text{sym}}(\rho_0)$ and L , the constraint from Sn neutron skin gives a negative correlation. This negative correlation is particularly interesting since combining it with other constraints will significantly improve the constraint on $E_{\text{sym}}(\rho_0)$ and L simultaneously. As pointed out by Zhang and Chen [49], the negative correlation can be understood from the fact that the neutron skin thickness of heavy nuclei is uniquely fixed by the symmetry energy slope $L(\rho)$ at a subsaturation cross density $\rho_c \approx 0.11 \text{ fm}^{-3}$ ($\approx 2/3\rho_0$) rather than at saturation density, and a fixed value of $L(\rho_c)$ can generally lead to a negative $E_{\text{sym}}(\rho_0)$ - $L(\rho_0)$ correlation [49].

Also included in Fig. 2 is a constraint from astrophysical observation based on Bayesian analysis on the currently available neutron star mass and radius measurements by Steiner and Gandolfi [57] (labeled “astrophysics”), for which a phenomenological parametrization for EOS of neutron matter near and above the saturation density is used with partial parameters determined by quantum Monte Carlo calculations. In addition, Fig. 2 also includes the results deduced from neutron matter constraints by Hebeler et al. (labeled “H”) [58] and by Gandolfi et al. [59] (labeled “G”). It is seen that the regions deduced from neutron matter deviate from the white region in Fig. 2 and this could be due to the fact that the higher-order contributions have been neglected in deducing the symmetry energy from pure neutron matter, as pointed out by Lattimer and Steiner [50]. It should be noted that although the empirical parabolic law works well for the evaluation of the symmetry energy magnitude, it might not be a good approximation for the calculation of the density slope of the symmetry energy for which the derivative with respect to the density is involved.

IV. NUCLEAR MATTER SYMMETRY ENERGY AT SUBSATURATION DENSITIES

In recent years, significant progress has been made in determining nuclear matter symmetry energy at subsaturation densities. In particular, it has been well established that the data of binding energy of finite nuclei can put rather stringent constraints on nuclear mat-

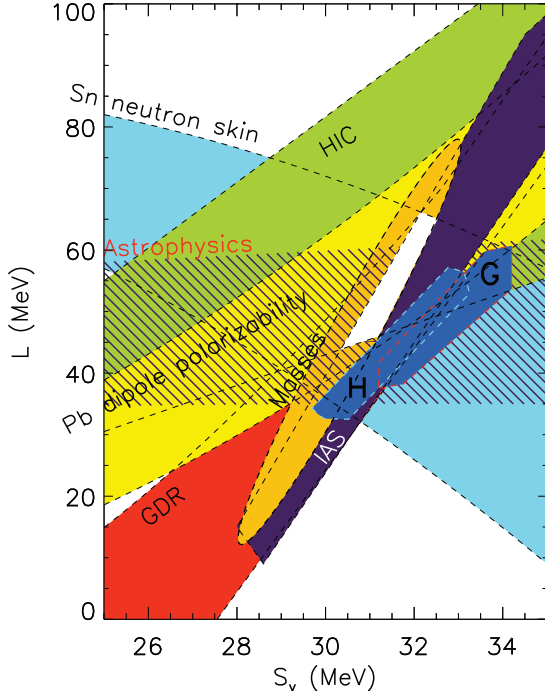


FIG. 2: (Color online) Constraints on symmetry energy slope parameter L and its magnitude S_v at ρ_0 from six experimental analyses and one astrophysical analysis. See the text for further discussion. G and H refer to the results from the neutron matter studies of Hebeler et al. [58] and Gandolfi et al. [59], respectively. Taken from Ref. [50].

ter symmetry energy at a subsaturation density $\rho \approx 2/3\rho_0$ [49, 56, 60–63]. It should be noted that a fixed value of $E_{\text{sym}}(\rho)$ at subsaturation density constrained from nuclear binding energy (nuclear mass) can generally lead to a positive $E_{\text{sym}}(\rho_0)$ - $L(\rho_0)$ correlation [48, 49], as observed in Fig. 2. For the symmetry energy at even lower densities around $\rho \approx \rho_0/3$, it has been shown recently [64] that the data of the electric dipole polarizability α_D in ^{208}Pb can put a quite accurate constraint. This can be easily understood from the following interesting relation [64]

$$\alpha_D(A) = \frac{e^2}{24} \frac{A \langle r^2 \rangle}{a_{\text{sym}} \left(\frac{27}{125} A \right)}, \quad (7)$$

which suggests that the α_D of a nucleus with mass number A is inversely proportional to the symmetry energy coefficient a_{sym} of a nucleus with mass number $(\frac{3}{5})^3 A$. For ^{208}Pb , one has $\alpha_D(A = 208) \propto 1/a_{\text{sym}}(A = 45)$. From the strong correlation between the $a_{\text{sym}}(A)$ and the $E_{\text{sym}}(\rho_A)$ at a specific density ρ_A [48, 56, 65, 66], the α_D in ^{208}Pb is thus expected to be strongly correlated with $E_{\text{sym}}(\rho)$ at $\rho = \rho_{A=45} \approx \rho_0/3$ [66].

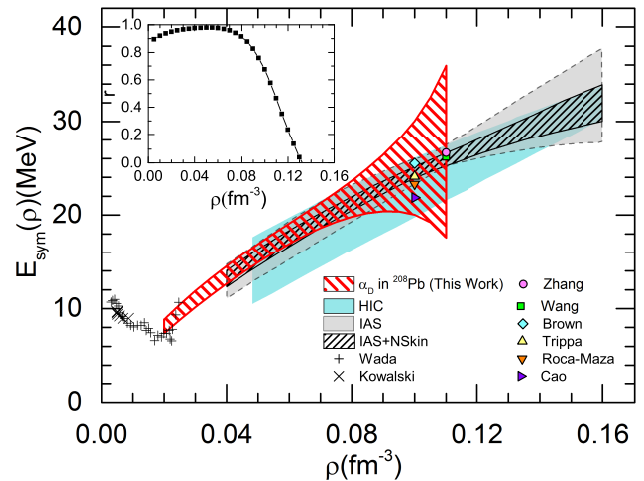


FIG. 3: (Color online) Constraints on the symmetry energy magnitude $E_{\text{sym}}(\rho)$ as a function of density ρ (see text for the details). The inset shows the density dependence of the Pearson correlation coefficient r between $1/\alpha_D$ in ^{208}Pb and the $E_{\text{sym}}(\rho)$. Taken from Ref. [64].

The red hatched band shown in Fig. 3 represents the constraints on the symmetry energy obtained from analyzing the data α_D in ^{208}Pb . Shown in the inset in Fig. 3 is the density dependence of the Pearson correlation coefficient r between the symmetry energy and the α_D in ^{208}Pb . At very low densities (i.e., less than about 0.02 fm^{-3}) where the fraction of light clusters becomes significant, clustering effects significantly increase the symmetry energy [67], and thus the constraints on the symmetry energy at densities below 0.02 fm^{-3} are not shown in Fig. 3 although the r value is still large. At higher densities (e.g., above 0.11 fm^{-3}), the r value becomes much smaller and effective constraints cannot be obtained.

Also shown in Fig. 3 are the constraints from transport model analyses of mid-peripheral heavy ion collisions of Sn isotopes (HIC) [55] and the SHF analyses of isobaric analogue states (IAS) as well as combining additionally the neutron skin “data” (IAS+NSkin) in Ref. [56], and six constraints on the value of $E_{\text{sym}}(\rho)$ around $2/3\rho_0$ from binding energy difference between heavy isotope pairs (Zhang) [49], Fermi-energy difference in finite nuclei (Wang) [62], properties of doubly magic nuclei (Brown) [63], the giant dipole resonance in ^{208}Pb (Trippa) [54], the giant quadrupole resonance in ^{208}Pb (Roca-Maza) [68] and the soft dipole excitation in ^{132}Sn (Cao) [69]. These constraints consistently favor a relatively soft symmetry energy or EOS of asymmetric nuclear matter at subsaturation densities.

Furthermore, Fig. 3 displays the experimental results of the symmetry energies at very low densities (below $0.2\rho_0$) with temperatures in the range $3 \sim 11 \text{ MeV}$ from the analysis of cluster formation in heavy ion collisions (Wada and Kowalski) [70]. It is interesting to see that

the constrained $E_{\text{sym}}(\rho)$ around $\rho_0/7$ from α_D in ^{208}Pb is nicely consistent with the results extracted from heavy ion collisions (Wada) which consider the clustering effects [70], and this feature seems to indicate that the clustering effects do not affect much the symmetry energy above about $\rho_0/7$ since the mean-field calculations of α_D in ^{208}Pb do not include the clustering effects. In addition, we note the $E_{\text{sym}}(\rho)$ has been predicted in microscopic calculations (see, e.g., Refs. [45, 71, 72]) and the results are consistent with the experimental constraints shown in Fig. 3.

V. NUCLEAR MATTER SYMMETRY ENERGY AT SUPRA-SATURATION DENSITIES

While the subsaturation density behaviors of nuclear matter symmetry energy have been relatively well-determined and considerable progress has been made on constraining the symmetry energy around the saturation density, the supra-saturation density behavior of the symmetry energy remains elusive and largely controversial. FOPI data on the π^-/π^+ ratio in heavy-ion collisions favor a quite soft symmetry energy at $\rho \geq 2\rho_0$ from the isospin and momentum dependent IBUU04 model analysis [26] while an opposite conclusion has been favored from the improved isospin dependent quantum molecular dynamics (ImIQMD) model analysis [27]. A recent analysis of FOPI π^-/π^+ ratio data based on the isospin dependent Boltzmann-Langevin approach [73] supported the conclusion of the IBUU04 model analysis. A careful check is definitely needed to understand the above model dependent conclusion. Recently, Xu *et al.* [74] explored the pion in-medium effect on the π^-/π^+ ratio in heavy-ion collisions at various energies within the framework of a thermal model, and they demonstrated that the pion in-medium effects reduce the π^-/π^+ ratio in heavy-ion collisions compared to that using free pions, especially at lower incident energies. Therefore, to understand quantitatively the symmetry energy effect on π^-/π^+ ratio in heavy-ion collisions, it is important to include the isospin-dependent pion in-medium effects [75, 76], although this is highly nontrivial in the implementation of the transport model simulations.

By analyzing the elliptic flow ratio of neutrons to protons or light nuclei from the FOPI/LAND data for $^{197}\text{Au} + ^{197}\text{Au}$ collisions at 400 MeV/nucleon within the UrQMD model, Russotto *et al.* [28] obtained a moderately soft symmetry energy with a density dependence of the potential part proportional to $(\rho/\rho_0)^\gamma$ with $\gamma = 0.9 \pm 0.4$, which is shown in Fig. 4 as a yellow band. In a more recent work, Cozma *et al.* [77] analyzed the FOPI/LAND data of neutron-proton elliptic flow difference and ratio for $^{197}\text{Au} + ^{197}\text{Au}$ collisions at 400 MeV/nucleon within the Tubingen QMD model by using a parametrization of the symmetry energy derived from the momentum dependent Gogny force, and they extracted a moderately stiff symmetry energy. Most

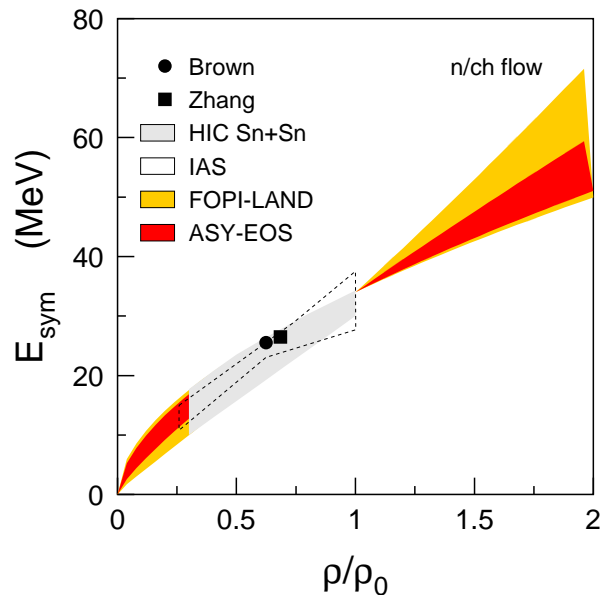


FIG. 4: (Color online) Constraints on the density dependence of the symmetry energy deduced from the FOPI-LAND result of Ref. [28] and the ASY-EOS result of Ref. [78]. The lower density results of Refs. [49, 55, 56, 63] are given by the symbols, the grey area (HIC), and the dashed contour (IAS). For clarity, the FOPI-LAND and ASY-EOS results are not displayed in the interval $0.3 < \rho/\rho_0 < 1.0$. Taken from Ref. [78].

recently, Russotto *et al.* [78] obtained a new and more stringent constraint on the symmetry energy for the regime of supra-saturation density with a considerably smaller uncertainty, i.e., $(\rho/\rho_0)^\gamma$ with $\gamma = 0.72 \pm 0.19$ (see the red band in Fig. 4), based on the UrQMD model analysis on the FOPI/LAND data of the elliptic flow ratio of neutrons to charged particles for $^{197}\text{Au} + ^{197}\text{Au}$ collisions at 400 MeV/nucleon. As shown in Fig. 4, this new constraint of a softer symmetry energy in the regime of supra-saturation density seems to be also consistent with the obtained constraints at subsaturation densities as shown in Fig. 3.

Besides using heavy ion collisions to constrain the supra-saturation density behavior of the symmetry energy, it has been also proposed recently [40] that the three bulk characteristic parameters $E_{\text{sym}}(\rho_0)$, L and the density curvature parameter $K_{\text{sym}} = 9\rho_0^2 \frac{d^2 E_{\text{sym}}(\rho)}{d\rho^2} |_{\rho=\rho_0}$ essentially determine the symmetry energy with the density up to about $2\rho_0$. This opens a new window to constrain the supra-saturation density behavior of the symmetry energy from its precise knowledge around saturation density.

VI. QUARK MATTER SYMMETRY ENERGY

The investigation of quark matter symmetry energy has been just started in recent years and there are

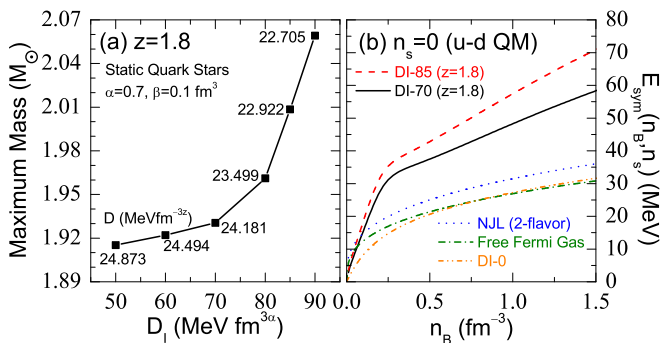


FIG. 5: (Color online) Left panel: D_I dependence of the maximum mass of static quark stars in the CIDDM model with $z = 1.8$. Right panel: The symmetry energy of two-flavor u - d quark matter as a function of baryon number density in the CIDDM model with DI-70 ($z = 1.8$) and DI-85 ($z = 1.8$). For comparison, the results of DI-0 as well as the symmetry energy of a free quark gas and normal quark matter within conventional NJL model are also included.

essentially no any empirical information on the density dependence of quark matter symmetry energy. Within the confined-isospin-density-dependent-mass (CIDDM) model [35], it has been shown recently that the isovector properties of quark matter may play an important role in determining the properties of strange quark matter and quark stars. In particular, if the recently discovered heavy pulsars PSR J1614-2230 [79] and PSR J0348+0432 [80] with mass around $2M_\odot$ were quark stars, they can put important constraint on the quark matter symmetry energy.

In the CIDDM model, the equivalent quark mass in isospin asymmetric quark matter with baryon density n_B and isospin asymmetry δ is parameterized as [35]

$$\begin{aligned} m_q &= m_{q_0} + m_I + m_{iso} \\ &= m_{q_0} + \frac{D}{n_B^z} - \tau_q \delta D_I n_B^\alpha e^{-\beta n_B}, \end{aligned} \quad (8)$$

where m_{q_0} is the quark current mass and $m_I = \frac{D}{n_B^z}$ reflects the isospin-independent part of the quark interactions in quark matter, z is the quark mass scaling parameter, D is a parameter determined by stability arguments of SQM; D_I , α , and β are parameters describing isospin dependence of the quark-quark effective interactions in quark matter, τ_q is the isospin quantum number of quarks and here we set $\tau_q = 1$ for $q = u$ (u quarks), $\tau_q = -1$ for $q = d$ (d quarks), and $\tau_q = 0$ for $q = s$ (s quarks). Shown in the left panel of Fig. 5 is the D_I dependence of the maximum mass of static quark stars. The value of the D parameter at different D_I shown in Fig. 5 corresponds to the value at which the quark star maximum mass becomes largest. It is seen from the left panel of Fig. 5 that the maximum mass of quark stars is sensitive to the D_I parameter and it increases with D_I . To obtain a quark star with mass larger than $1.93M_\odot$, we find the minimum

value of D_I should be $70 \text{ MeV} \cdot \text{fm}^{3\alpha}$, and the corresponding parameter set is denoted as DI-70 ($z = 1.8$). For DI-70 ($z = 1.8$), we have $D_I = 70 \text{ MeV} \cdot \text{fm}^{3\alpha}$, $\alpha = 0.7$, $\beta = 0.1 \text{ fm}^3$, $D = 24.181 \text{ MeV} \cdot \text{fm}^{-3z}$, and $z = 1.8$.

Shown in the right panel of Fig. 5 is the density dependence of two-flavor u - d quark matter symmetry energy in the CIDDM model with DI-70 ($z = 1.8$). For comparison, we also include the results of the DI-85 ($z = 1.8$) parameter set (which produces a quark star mass of $2.01M_\odot$), the DI-0 parameter set (i.e., $D_I = 0$) as well as the symmetry energy of a free quark gas (with $m_{u0} = m_{d0} = 5.5 \text{ MeV}$) and normal quark matter within conventional Nambu-Jona-Lasinio (NJL) model [81]. One can see that the DI-0 and NJL model predict a very similar quark matter symmetry energy as that of the free quark gas, while the DI-70 ($z = 1.8$) parameter set predicts a two times larger quark matter symmetry energy than the free quark gas. Our results thus indicate that the two-flavor u - d quark matter symmetry energy should be at least about twice that of a free quark gas or normal quark matter within conventional NJL model in order to describe the PSR J1614-2230 and PSR J0348+0432 as quark stars. It should be mentioned that the symmetry energy of two-flavor color superconductivity (2SC) phase is about three times that of the normal quark matter phase [33], and thus is close to the symmetry energy predicted by DI-70 ($z = 1.8$).

VII. SUMMARY

We have given a brief overview of the current status on the symmetry energy in nuclear and quark matter. For nuclear matter, considerable progress has been made in determining the density dependence of nuclear matter symmetry energy during the last decade due to the great efforts from experiments, astrophysical observations and theoretical calculations in the community. Very encouragingly, one can see that the various constraints on the symmetry energy at subsaturation densities are consistently convergent and the symmetry energy values at subsaturation densities have been constrained with good precision. Around saturation density, although the values of the symmetry energy magnitude $E_{\text{sym}}(\rho_0)$ and its density slope L at saturation density can vary largely depending on the data or models, all the constraints obtained so far from nuclear reactions, nuclear structures, and the properties of neutron stars are consistent with $E_{\text{sym}}(\rho_0) = 32.5 \pm 2.5 \text{ MeV}$ and $L = 55 \pm 25 \text{ MeV}$. On the other hand, all the constraints on nuclear matter symmetry energy at supra-saturation densities have been obtained from analyzing data in heavy-ion collisions within transport models, and these constraints are largely controversial. More high quality data and more accurate theoretical methods are definitely needed to further reduce the theoretical and experimental uncertainties of the constraints on the density dependence of nuclear matter symmetry energy.

The quark matter symmetry energy is a new topic and it may play an important role in understanding properties of isospin asymmetric quark matter, which could be formed or exist in ultra-relativistic heavy-ion collisions induced by neutron-rich nuclei and in the interior of neutron stars or quark stars. Based on a quark matter model, i.e., the confined-isospin-density-dependent-mass model, it has been shown that if the recently discovered pulsars with two times solar mass were quark stars, the two-flavor u - d quark matter symmetry energy should be at least about twice that of a free quark gas or normal quark matter within conventional NJL model. This result indicates that the u and d quarks could feel very different interactions in isospin asymmetric quark matter, which may have important implications on the isospin effects of partonic dynamics in heavy-ion collisions at ultra-relativistic energies, e.g., at RHIC in USA, FAIR in Germany, and NICA in Russia.

Acknowledgments

The author would like to thank Bao-Jun Cai, Rong Chen, Peng-Cheng Chu, Wei-Zhou Jiang, Che Ming Ko,

Bao-An Li, Kai-Jia Sun, Rui Wang, Xin Wang, De-Hua Wen, Zhi-Gang Xiao, Chang Xu, Jun Xu, Gao-Chan Yong, Zhen Zhang, and Hao Zheng for fruitful collaboration and stimulating discussions. This work was supported in part by the Major State Basic Research Development Program (973 Program) in China under Contract Nos. 2013CB834405 and 2015CB856904, the National Natural Science Foundation of China under Grant Nos. 11625521, 11275125 and 11135011, the Program for Professor of Special Appointment (Eastern Scholar) at Shanghai Institutions of Higher Learning, Key Laboratory for Particle Physics, Astrophysics and Cosmology, Ministry of Education, China, and the Science and Technology Commission of Shanghai Municipality (11DZ2260700).

-
- [1] LI B A, KO C M, BAUER W, *Int. J. Mod. Phys. E* **7**, 147 (1998).
- [2] LATTIMER J M, PRAKASH M, *Science* **304**, 536 (2004); *Phys. Rep.* **442**, 109 (2007).
- [3] STEINER A W, PRAKASH M, LATTIMER J M, *et al.*, *Phys. Rep.* **411**, 325 (2005).
- [4] BARAN V, COLONNA M, GRECO V, *et al.*, *Phys. Rep.* **410**, 335 (2005).
- [5] CHEN L W, KO C M, LI B A *et al.*, *Front. Phys. China*, **2**, 327 (2007) [arXiv:0704.2340].
- [6] LI B A, CHEN L W, KO C M, *Phys. Rep.* **464**, 113 (2008).
- [7] TRAUTMAN W, WOLTER H H, *Int. J. Mod. Phys. E* **21**, 1230003 (2012).
- [8] TSANG B M, STONE J R, CAMERA F, *et al.*, *Phys. Rev. C* **86**, 015803 (2012).
- [9] LATTIMER J M, *Ann. Rev. Nucl. Part. Sci.* **62**, 485 (2012).
- [10] LI B A, CHEN L W, FATTOYEV F J, *et al.*, *J. Phys.: Conf. Series* **413**, 012021 (2013) [arXiv:1212.1178].
- [11] LI B A, RAMOS A, VERDE G, VIDANA I, *Eur. Phys. Journal A* **50**, (2014).
- [12] HOROWITZ C J, BROWN E F, KIM Y, *et al.*, *J. Phys. G* **41**, 093001 (2014).
- [13] CHEN L W, *Nucl. Phys. Rev.* **37**, 273 (2014) [arXiv:1212.0284].
- [14] WANG R, CHEN L W, *Phys. Rev. C* **92**, 031303(R) (2015).
- [15] BALDO M, BURGIO G F, *Prog. Part. Nucl. Phys.* **91**, 203 (2016).
- [16] LI Z, *Nucl. Phys. Rev.* **31**, 285 (2014).
- [17] JIANG W, YANG R, ZHANG D, *Nucl. Phys. Rev.* **31**, 333 (2014).
- [18] DONG J, ZUO W, GU J, *et al.*, *Nucl. Phys. Rev.* **31**, 429 (2014).
- [19] WU Q, ZHANG Y, XIAO Z, *et al.*, *Nucl. Phys. Rev.* **33**, 251 (2016).
- [20] WANG H, XU C, *Nucl. Phys. Rev.* **33**, 1 (2016).
- [21] HOROWITZ C J, POLLOCK S J, SOUDER P A, *et al.*, *Phys. Rev. C* **63**, 025501 (2001).
- [22] SIL T, CENTELLES M, VIÑAS, *et al.*, *Phys. Rev. C* **71**, 045502 (2005).
- [23] WEN D H, LI B A, CHEN L W, *Phys. Rev. Lett.* **103**, 211102 (2009).
- [24] ZHENG H, ZHANG Z, CHEN L W, *J. Cosmo. Astropart. Phys.* **08**, 011 (2014).
- [25] CARLSON J, GANDOLFI S, PEDERIVA F, *et al.*, *Phys. Rev. C* **87**, 1067 (2015).
- [26] XIAO Z G, LI B A, CHEN L W, *et al.*, *Phys. Rev. Lett.* **102**, 062502 (2009).
- [27] FENG Z Q, JIN G M, *Phys. Lett.* **B683**, 140 (2010).
- [28] RUSSOTTO P, WU P Z, ZORIC M, *et al.*, *Phys. Lett.* **B697**, 471 (2011).
- [29] XU C, LI B A, *Phys. Rev. C* **81**, 064612 (2010).
- [30] WANG Y, GUO C, LI Q, *et al.*, *Nucl. Phys. Rev.* **32**, 154 (2015).
- [31] DI TORO M, BARAN V, COLONNA M, *et al.*, *Nucl. Phys.* **A775**, 102 (2006).
- [32] DI TORO M, BARAN V, COLONNA M, GRECO V, *J. Phys. G* **37**, 083101 (2010).
- [33] PAGLIARA G, SCHAFFNER-BIELICH J, *Phys. Rev. D* **81**, 094024 (2010).
- [34] SHAO G Y, COLONNA M, DI TORO M, *et al.*, *Phys. Rev. D* **85**, 114017 (2012).
- [35] CHU P C, CHEN L W, *Astrophys. J.* **780**, 135 (2014).
- [36] LIU H, XU J, CHEN L W, SUN K J, *Phys. Rev. D* **94**,

- 065032 (2016).
- [37] XIA Y H, XU C, ZONG H S. 2016 [arXiv:1608.01724].
- [38] CAI B J, CHEN L W, Phys. Rev. C **85**, 024302 (2012).
- [39] ROCA-MAZA X, CENTELLES M, VINAS X, WARDA M, Phys. Rev. Lett. **106**, 252501 (2011).
- [40] CHEN L W. EPJ Web Conf. **88**, 00017 (2015) [arXiv:1506.09057].
- [41] VIDANA I, PROVIDENCIA C, POLLS A, RIOS A, Phys. Rev. C **80**, 045806 (2009).
- [42] LI Z H, SCHULZE H J, Phys. Rev. C **78**, 028801 (2008).
- [43] KLAHN T, BLASCHKE D, TYPEL S, *et al.*, Phys. Rev. C **74**, 035802 (2006).
- [44] SAMMARRUCA F, Int. J. Mod. Phys. E **19**, 1259 (2010).
- [45] AKMAL A, PANDHARIPANDE V R, RAVENHALL D G, Phys. Rev. C **58**, 1804 (1998).
- [46] FRIEDMAN B, PANDHARIPANDE V R, Nucl. Phys. **A361**, 502 (1981).
- [47] WIRINGA R B, FIKS V, FABROCINI A, Phys. Rev. C **38**, 1010 (1988).
- [48] CHEN L W, Phys. Rev. C **83**, 044308 (2011).
- [49] ZHANG Z, CHEN L W, Phys. Lett. **B726**, 234 (2013).
- [50] LATTIMER J M, STEINER A W, Eur. Phys. J. A **50**, 40 (2014).
- [51] KORTELAINEN M, LESINSKI T, MORE J, *et al.*, Phys. Rev. C **82**, 024313 (2010).
- [52] CHEN L W, KO C M, LI B A, XU J, Phys. Rev. C **82**, 024321 (2010).
- [53] TAMII A, POLTORATSKA I, von NEUMANN-COSEL P, *et al.*, Phys. Rev. Lett. **107**, 062502 (2011).
- [54] TRIPPA L, COLO G, VIGEZZI E, Phys. Rev. C **77**, 061304 (2008).
- [55] TSANG M B, ZHANG Y X, DANIELEWICZ, *et al.*, Phys. Rev. Lett. **102**, 122701 (2009).
- [56] DANIELEWICZ P, LEE J, Nucl. Phys. **A922**, 1 (2014).
- [57] STEINER A W, GANDOLFI S, Phys. Rev. Lett. **108**, 081102 (2012).
- [58] HEBELER K, LATTIMER J, PETHICK C, *et al.*, Phys. Rev. Lett. **105**, 161102 (2010).
- [59] GANDOLFI S, CARLSON J, REDDY S, Phys. Rev. C **85**, 032801(R) (2012).
- [60] HOROWITZ C J, PIEKAREWICZ J, Phys. Rev. Lett. **86**, 5647 (2001).
- [61] FURNSTAHL R J, Nucl. Phys. **A706**, 85 (2002).
- [62] WANG N, OU L, LIU M, Phys. Rev. C **87**, 034327 (2013).
- [63] BROWN B A, Phys. Rev. Lett. **111**, 232502 (2013).
- [64] ZHANG Z, CHEN L W, Phys. Rev. C **92**, 031301(R) (2015).
- [65] CENTELLES M, ROCA-MAZA X, VINAS X, *et al.*, Phys. Rev. Lett. **102**, 122502 (2009); WARDA M, VINAS X, ROCA-MAZA X, *et al.*, Phys. Rev. C **80**, 024316 (2009).
- [66] ALAM N, AGRAWAL B K, DE J N, *et al.*, Phys. Rev. C **90**, 054317 (2014).
- [67] TYPEL S, ROPKE G, KLAHN T, *et al.*, Phys. Rev. C **81**, 015803 (2010).
- [68] ROCA-MAZA X, BRENNA M, AGRAWAL B K, *et al.*, Phys. Rev. C **87**, 034301 (2013).
- [69] CAO L G, MA Z Y, Chin. Phys. Lett. **25**, 1625 (2008).
- [70] NATOWITZ J B, ROPKE G, TYPEL S, *et al.*, Phys. Rev. Lett. **104**, 202501 (2010); KOWALSKI S, NATOWITZ J B, SHLOMO S, *et al.*, Phys. Rev. C **75**, 014601 (2007); WADA R, HAGEL K, QIN L, *et al.*, Phys. Rev. C **85**, 064618 (2012).
- [71] DRISCHLER C, SOMA V, SCHWENK A, Phys. Rev. C **89**, 025806 (2014).
- [72] WELLENHOFER C, HOLT J W, KAISER N, Phys. Rev. C **92**, 015801 (2015).
- [73] XIE W J, SU J, ZHU L, ZHANG F S, Phys. Lett. **B718**, 1510 (2013).
- [74] XU J, CHEN L W, KO C M, *et al.*, Phys. Rev. C **87**, 067601 (2013).
- [75] HONG J, DANIELEWICZ P, Phys. Rev. C **90**, 024605 (2014).
- [76] SONG T, KO C M, Phys. Rev. C **91**, 014901 (2015).
- [77] COZMA M D, LEIFELS Y, TRAUTMANN W, *et al.*, Phys. Rev. C **88**, 044912 (2013).
- [78] RUSSOTTO P, GANNON S, KUPNY S, *et al.*, Phys. Rev. C **94**, 034608 (2016).
- [79] DEMOREST P, PENNUCCI T, RANSOM, S, *et al.*, Nature **467**, 1081 (2010).
- [80] ANTONIADIS J, FREIRE P C C, WEX N, *et al.*, Science **340**, 6131 (2013).
- [81] REHBERG P, KLEVANSKY S P, HUFNER J, Phys. Rev. C **53**, 410 (1996).